JOURNAL OF MATERIALS SCIENCE: MATERIALS IN MEDICINE **15** (2004) 1261 – 1266

Phase development and structural characterization of calcium phosphate ceramics-polyacrylic acid nanocomposites at room temperature in water-methanol mixtures

SZ-CHIAN LIOU[1], SAN-YUAN CHEN[1,*], DEAN-MO LIU[2]
[1]*Department of Materials Science and Engineering, National Chiao Tung University, 1001 Ta-hsueh Rd., Hsinchu, Taiwan 300, Republic of China*
E-mail: sychen@cc.nctu.edu.tw
[2]*ApaMatrix Technologies Inc., 58-7151 Moffatt Road, Richmond, British Columbia, Canada V6Y3G9*

Calcium phosphate ceramics (CPCs) were prepared via an *in-situ* formation in the presence of polyacrylic acid (PAA) polymer under water-methanol (WM) mixture at room temperature. The PAA polymer was employed as both structure-directing agent and crystallization retardant to manipulate the development of resulting CPCs nano-crystallites which are observed to show a core-shell configuration with a thin layer of PAA molecules. A resulting phase evolution map with respect to the developing phases of calcium-deficient hydroxyapatite (CDHA), β-tricalcium phosphate (β-TCP), and an intermediate amorphous calcium phoshate (ACP) that were structurally and spectroscopically identified, was constructed in terms of fractions of water-to-methanol proportions and concentration of PAA. It is found that for the solutions in both water-rich and methanol-rich regions, pure CDHA and β-TCP instead of intermediate ACP phase can be developed irrespective of the concentration of PAA, respectively. For conditions in between, i.e., with methanol fractions of 15%–90%, ACP appeared only when the PAA fell in a limited concentration range.

1. Introduction

Calcium phosphate ceramics (CPCs) have long been received a great deal of attention as prime candidates for a number of biomedical applications such as orthopedics, dentistry and drug delivery, simply because they exhibit considerably improved biological affinity and activity, compared to currently existing synthetic materials, to surrounding host tissues when implanted. Among those CPCs, particular attention has been placed to hydroxyapatite $Ca_{10}(PO_4)_6(OH)_2$ (HA) and beta-tricalcium phosphate β-$Ca_3(PO_4)_2$ (β-TCP) due to their outstanding biological responses to physiological environments [1]. On the other hand, the calcium-deficient apatites [$Ca_{10-x}(PO_4)_{6-x}(HPO_4)_x(OH)_{2-x}$, $0 \leq x \leq 1$, CDHA] are of greater biological interest than both HA and β-TCP because of chemically and structurally closer to natural bones [2].

Natural biomaterials exhibit nanostructured with a needle-like or rod-like shape well arranged within the polymeric matrix, e.g., collagen, to form natural bone. Most critically, biomaterials exhibit excellent metabolic activity even when subject to subtle environmental changes, compared to those synthetic biomaterials [1]. Recently, it is more advanced to use different methodologies to form nano-crystal-contained composites (or termed nanocomposites) at ambient temperature, for a variety of biomedical applications [3–5]. Among those existing methodologies, *in-situ* formation of the nanocomposites by forming the nano-CPCs crystals in the presence of polymers is one of most attractive routes, since it avoids extensive particle agglomeration if a mechanical mixing between nanopowder and selected polymer was adapted. Although the *in-situ* formation of the HA-polymer nanocomposites in water has been described in the literature [3–5], no detailed nanostructure and phase evolution were analyzed. Furthermore, *in-situ* formation CPCs-polymer nanocomposites in the water-alcohol mixtures has been never systematically studied and reported in view of the literature.

Water-alcohol mixtures have frequently been considered as interesting media due to their anomalous behavior in terms of such as a spectrum of viscosity-composition profile and negatively relative partial

*Author to whom all correspondence should be addressed.

volume, and this is often explained in terms of competition between different hydration effects. Of the aqueous alcohols, methanol has been the most thoroughly studied because it has a very signification effect on water structure due to hydrophobic hydration effects. Thus it is plausible to expect that it may change in solvent structure [6]. In an attempt to understand the hydrophobic effect on the synthesis of CPCs [7], Lerner *et al.* reported that different crystalline degree of HA powders, from amorphous to well-crystallized structure, can be synthesized with various ethanol/water ratios [8]. However, the role of polymer addition in the phase evolution of CPCs has not been investigated in the water-methanol mixtures.

In the integral part of whole project to be elucidated in this present, we focus on the *in-situ* synthesis of composite-type nanocrystal calcium phosphate bioceramics, instead of pure inorganic crystals as frequently reported, in water-methanol mixtures at ambient temperature. The phase evolution and microstructure analysis will be also studied to clarify the importance of polyacrylic acid (PAA) addition in the nanocomposites.

2. Experimental procedure

The starting materials used in this investigation are analytical-grade $(CH_3COO)_2Ca{\cdot}xH_2O$ (99%, Aldrich Chemical company, Inc., USA) which is used as the Ca source, and H_3PO_4 (85%, Riedel-deHaen, Seelze, Germany) as the P source. After dissolving 0.015 mole $(CH_3COO)_2Ca{\cdot}xH_2O$ in different deionized water/anhydrous methanol (Merck) volume ratio, Poly (acrylic acid) (Mw 2000) (PAA, Aldrich Chemical company, Inc., USA) was added to the solution and adjusted the solution to the pH value of 9 using 5 M NaOH solution. Phosphoric acid (0.01 mole) was then dropped into the above solution and at the same time, the sodium hydroxide solution was used to keep the solution at pre-determined pH value throughout the entire synthesis process. All the procedures were processed at room temperature (25 °C) and following an ageing time period of 16 h. After filtering and washing with deionized water several times, white precipitated powder, having a Ca/P ratio of 1.5 as spectroscopically determined, was finally obtained after drying overnight at 80 °C.

X-ray diffractometry (M18XHF, MAC Science, Tokyo, Japan) was used for identifying the crystalline phase of the synthesized compounds at a 4° 2θ/min from 20 to 60 °. Fourier transform Infrared ray (FT-IR) spectra were performed using KBr pellets (2 mg per 300 mg KBr) on a spectrometer (Model 580, Perkin-Elmer) with a resolution of 4.00 cm^{-1}. Infrared spectra were recorded in the range of 4000–400 cm^{-1} to evaluate the molecular structure and phase clarification of the resulting powders.

The powder sample was ultrasonically dispersed in acetone to form very dilute suspensions and a few droplets were then dropped on copper grids with carbon film coated. Microstructure observations were performed in Philips Tecnai 20 (Holland, The Nertherlands) microscope operating at 200 keV.

3. Results and discussion

3.1. Phase identification and evolution

The XRD patterns in Fig. 1 show a poorly-crystalline calcium-deficient apatite (CDHA) phase according to ICDD No. 9–432 as the synthetic CPCs powders with different concentrations of PAA were formed in pure water. Furthermore, it is interesting to note that with increasing PAA concentration, the diffraction intensity decreases, revealing that the crystallization of apatitic crystals was highly retarded in the presence of PAA [5].

Fig. 2 shows the XRD patterns of the synthetic powders in the 50–50% water-methanol (WM) solution at different PAA concentrations. It was observed that when the PAA concentration is less than 0.01 wt% or more than 0.1 wt%, the synthetic powders were identified as the CDHA phase. However, as the added PAA concentration is in the range of 0.01–0.1 wt%, a broad peak as calibrated by external standard of Si powder was found near 31 ° instead of 32 ° (a characteristic reflection position of stoichiometry HA). Similar peak

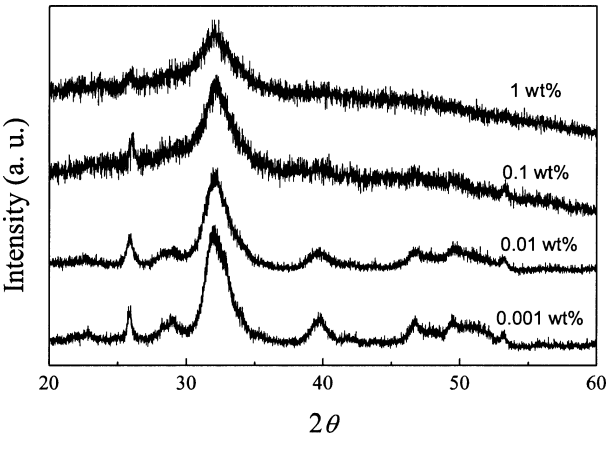

Figure 1 X-ray diffraction patterns of the calcium phosphate powders with different PAA concentrations in pure water.

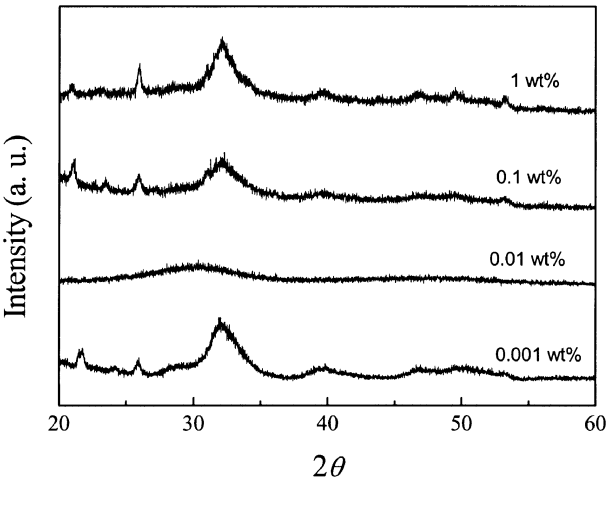

Figure 2 X-ray diffraction patterns of the calcium phosphate powders with different PAA concentrations in the 50–50% water-methanol mixture.

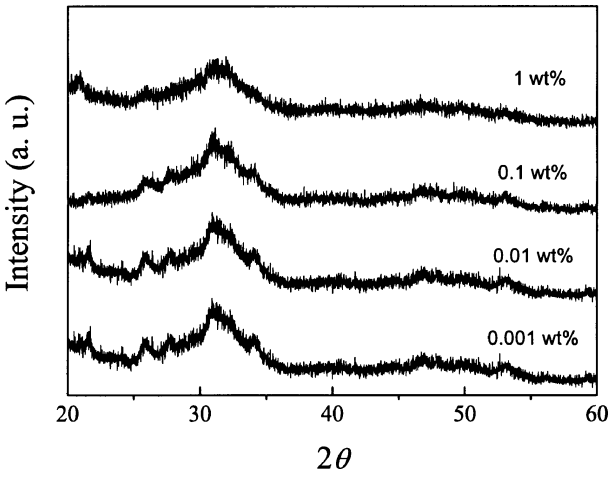

Figure 3 X-ray diffraction patterns of the calcium phosphate powders with different PAA concentrations in pure methanol.

was also observed by Lerner et al. and considered as an amorphous phase $Ca_3(PO_4)_2 \cdot xH_2O$ in the water-ethanol mixtures [8].

If pure anhydrous methanol was used as solvent to study the phase evolution of the resulting CPCs crystals, Fig. 3 shows that with different PAA concentrations, the resulting crystalline phase can be identified as β-tricalcium phosphate (β-TCP) according to ICDD No. 9–169. Furthermore, the diffraction intensity of the β-TCP decreases with an increase of PAA concentration in anhydrous methanol, which is similar to that of Fig. 1 in pure water.

In order to identify the molecular arrangement of the precipitate powders, Fourier Transform Infrared Ray (FT-IR) analysis was performed. Fig. 4 illustrates that the FT-IR spectra of CDHA, ACP and β-TCP powders. It was observed that no apparent differences in the absorption peaks among CDHA, β-TCP and ACP can be detected. It clearly shows the presence of two characteristic v_4 PO_4 bands at around 563 cm^{-1} and 600 cm^{-1}, and v_3 PO_4 band in the range of 1100–1000 cm^{-1} in all the cases, which are characteristic of molecular structure in the apatitic lattice [9]. The presence of bands at 1115, 1096, 1007 and 944 cm^{-1} can be assigned to groups of β-TCP [10]. The bands in the range of 1750 cm^{-1} −1450 cm^{-1} are assigned to the characteristic absorption peaks of PAA molecules. Those aforementioned absorption peaks indicate that the powders prepared in this study were virtually a mixture of CDHA or β-TCP crystals together with PAA. These broad, featureless PO_4^{3-} stretching and bending modes (v_3 and v_4 bands) between 1092–1040 cm^{-1} and 462–474 cm^{-1} also suggest that the resulting crystals exhibit amorphous structure, in agreement with XRD results. The splitting of the degenerate PO_4^{3-} v_3 and v_4 bands at 462–474 cm^{-1} and 1092–1040 cm^{-1} gradually appears in the CDHA and β-TCP crystal. This observation appears to be a result of site-symmetry splitting of the degenerate modes as the environment of the PO_4^{3-} groups becomes more structurally [8, 11]. Molecular and adsorbed water bands are also discerned at 1640 cm^{-1} and 3400 cm^{-1}. Furthermore, comparison of the FT-IR spectra of ACP with CDHA and β-TCP demonstrates that ACP contains a higher amount of water at 3400 cm^{-1}. It seems to indicate that there are numerous hydroxyl group molecules in the ACP structure in the WM mixtures.

3.2. Phase evolution map

The PAA concentration on the phase formation of the synthetic powders with various WM ratios investigated in this work is summarized in Fig. 5. It seems to reveal that the presence of methanol does influence the phase evolution of CDHA over a wide range of concentration from 15 to 100%. The map of phase evolution can generally be interpreted from the following three aspects: (1) pure water, (2) pure methanol and (3) water-methanol mixture.

3.2.1. Pure water

In previous study, the CDHA can be easily obtained in pure water with or without the presence of PAA [5, 9]. It is concluded from the current and previous work that the role of polyelectrolyte, PAA, is likely identical regardless of the molecular weight on phase evolution in pure water. Accordingly, an increase in the

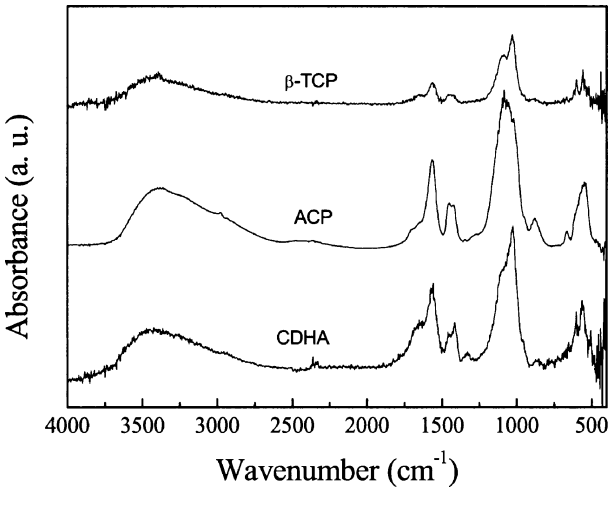

Figure 4 FT-IR spectra of the CDHA, ACP and β-TCP powders.

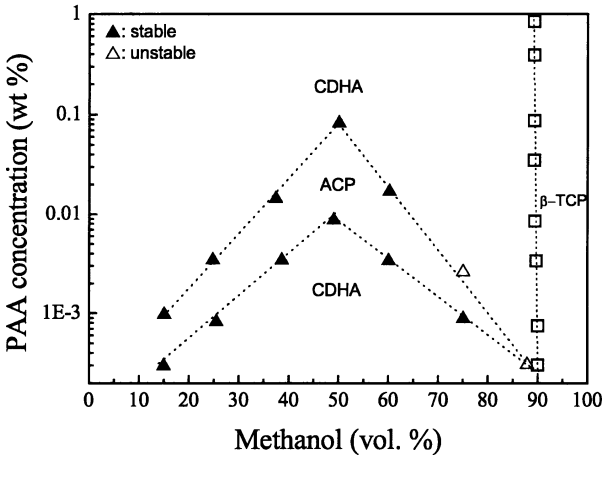

Figure 5 Phase evolution map of the calcium phosphate powders with various WM ratios and PAA concentrations.

PAA concentration indicates an increase in amount of dissociated PAA anions, i.e., carboxylic ion $(COO)^-$, in water that may be described as Equation 1 [3–5, 12, 13].

$$PAA \leftrightarrow PAA(COO)^- + H^+ \quad (1)$$

Since the solutions remain optically clear after Ca ions were mixed with PAA polymer solution and no sign of precipitate or visible colloidal complex can be optically detected, a further association of $PAA(COO)^-$ and Ca^{++} results in a Ca-PAA(COO) complex can be described by Equation 2.

$$PAA(COO)^- + Ca^{2+} \leftrightarrow PAA(COO)Ca^+ \quad (2)$$

As reported in the literature [3], a Ca-PAA(COO) complex was rapidly formed in aqueous solution which inhibits further reaction between available Ca ions and phosphate ions to form crystalline apatite. Therefore, the nucleation and growth of the CDHA crystals will be retarded and CDHA can be only observed in the studied range. However, the crystallinity of CDHA is getting poor with increasing PAA concentration.

3.2.2. Pure methanol

Fig. 6 illustrates the XRD patterns of the CPC synthesized in methanol containing 0.01 wt% PAA. The developing crystals evolve with a phase change from $CaHPO_4$, ACP1 ($Ca_9(PO_4)_6$-like structure), ACP2 (TCP-like structure) to β-TCP with increasing time of aging in the solution as reported in our previously results [11]. The β-TCP will finally become a stable phase at the end of synthesis. Furthermore, it is ascertained that the resulting powders are virtually a mixture of inorganic β-TCP crystals and organic PAA in the pure methanol, as evidenced from the FT-IR analysis depicted in Fig. 4. It seems to imply that an interaction exists between PAA molecules and methanol. The PAA molecules can be dissolved in methanol termed as alcoholyzation. In contrast to pure water, the visible colloidal complex appears in the solutions and

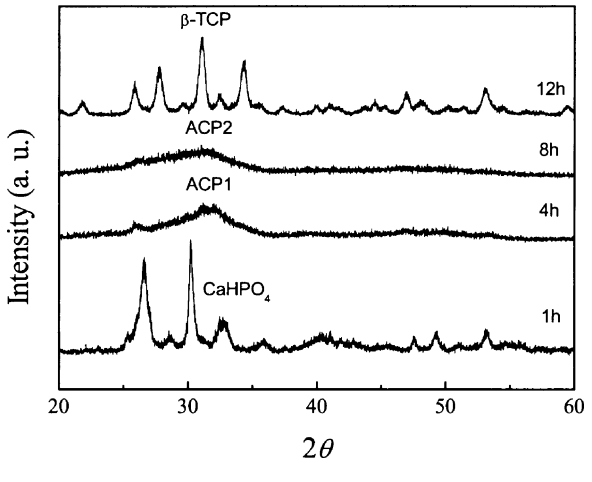

Figure 6 X-ray diffraction patterns for the phase development of calcium phosphate powders with aging time in methanol containing 0.01 wt% PAA.

can be visually detected after the Ca-methanol solution was mixed with the PAA-methanol solution. The interaction between PAA molecules and Ca ions results in an amorphous Ca-PAA complex that further suppresses the desired reaction between Ca and P to form crystalline phase such as β-TCP, and this is evidenced with the XRD results (Fig. 3). Therefore, it can be concluded that the PAA polymer is likely to play the same role in retarding the nucleation and growth of the corresponding crystals in methanol as well as in water.

3.2.3. Water-methanol mixtures

According to above discussion, PAA polymer plays the same role in retarding the nucleation and growth of crystalline particles such as CDHA or β-TCP in both water and methanol. However, in water-methanol mixtures, a greater tendency of the formation of ACP phase is observed over a certain range PAA concentration with methanol fractions ranging from 15 to 90%. It seems to imply that some interactions exist between water and methanol where exerts higher interference on phase evolution than the PAA effect alone. In the literature, it has been reported that the hydrophobic hydration structure such as clathrate-like cage will be constructed around the alcohol group in the water-alcohol mixtures [8, 14, 15]. By applying the same concept in this work, if this hydrophobic hydration structure does exist in the water-alcohol mixtures, it will retard the nucleation of crystalline phase. At low fractions of methanol, e.g. 25%, the hydrophobic hydration causes strong hydration sphere around Ca ions and it becomes difficult to overcome the energy barrier of dehydration to form the stable crystalline phase. Furthermore, the dissolution rate of PAA in methanol is faster than that in water (as experimentally observed) and thus, this hydrophobic hydration structure may sustain even at a low PAA concentration. However, with higher PAA concentration, the effect of hydrophobic hydration in the WM solution becomes smaller. Consequently, the ACP was formed when the added PAA concentration is lying between 0.005 and 0.01 wt% at a low fraction of methanol. With further increasing methanol up to 50%, most of the PAA molecules tend to react with methanol. Therefore, the hydrophobic hydration structure was constructed again for PAA concentration between 0.005 and 0.1 wt%, and thus, ACP was formed. On the other hand, for PAA concentration <0.005 wt%, the CDHA crystals can be easily developed because the retardation of PAA molecules on the nucleation and growth of CDHA crystals is reduced. However, for PAA concentration >0.1 wt%, the CDHA was formed again because of no available methanol molecules present to form hydrophobic hydration structure. Therefore, the CDHA crystals with different aspect ratio can be developed from the different PAA regions (not shown here). If further increasing methanol over 75%, the hydrophobic hydration structure becomes unstable and tends to be broken down. Therefore, it is difficult to form ACP structure in the media with small fraction of water. As shown in Fig. 5, when 90% methanol was used, only CDHA phase was detected and the ACP phase then disappeared.

3.3. Phase morphology and analysis

Fig. 7(a) and (b) shows the TEM bright-field (BF) image of the synthetic CDHA powders in pure water with PAA concentrations of 0.01 and 1 wt%, respectively. With PAA concentration of 0.01 wt%, the CDHA crystal has dimensions of 2–5 nm in diameter and 50–70 nm in length. Furthermore, the needle-shape CDHA was surrounding with a thin amorphous layer as shown in the inset of Fig. 7(a) to form core-shell structure. However, as increasing PAA concentration to 1 wt%, the CDHA morphology changes from needle-like shape to spherical shape with 40 nm in diameter. The spherical CDHA nanocrystals, marked with arrows, were surrounded in the PAA matrix. It seems to imply that the PAA molecular suppresses the CDHA growth direction and modifies its shape from needle to sphere if the added PAA concentration is more than 1 wt% in the solution.

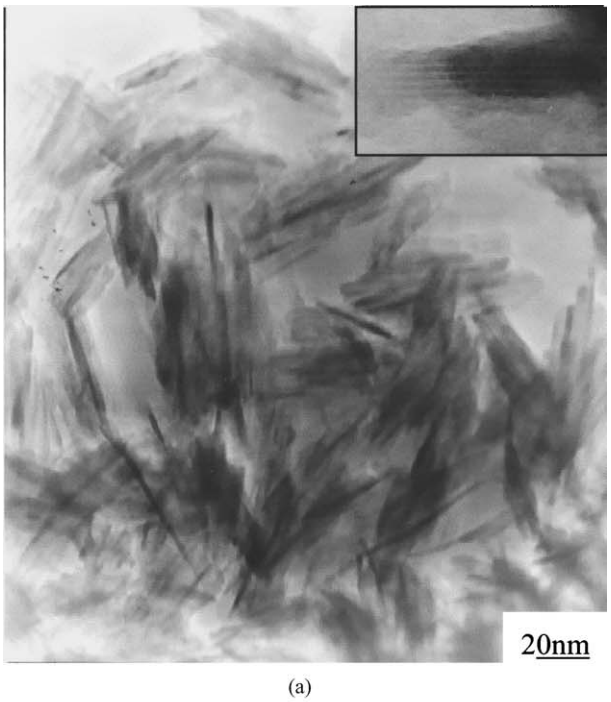

(a)

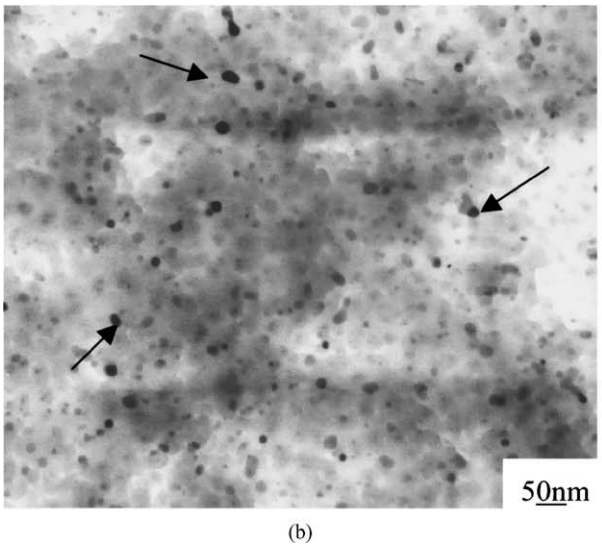

(b)

Figure 7 TEM bright-field (BF) image of CDHA in pure water: (a) 0.01 wt% PAA and (b) 1 wt% PAA.

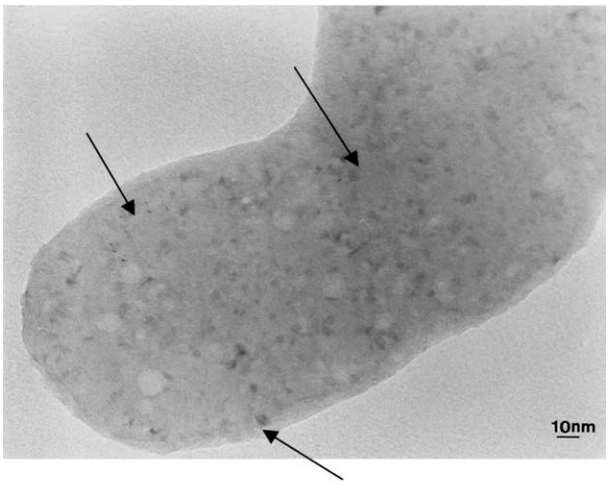

(a)

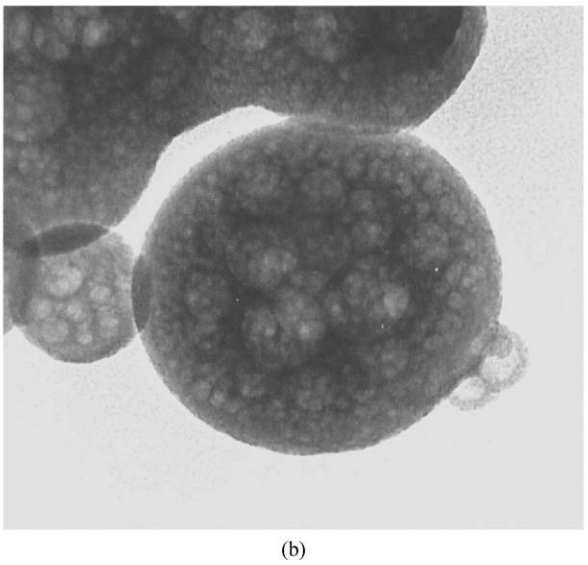

(b)

Figure 8 High resolution TEM image of ACP.

Two different microstructures of ACP were observed in this investigation. One is composed of agglomerates with the primary particles of 2–5 nm in diameter as marked with the arrows (Fig. 8(a)), and the other is a continuous random network structure (Fig. 8(b)). However, with these structures, it shows a higher specific surface area and the hydroxyl group is easily trapped on the surface of ACP as demonstrated by FT-IR spectra. It seems to reveal that adsorbed alcohol molecules stabilize ACP although the ACP, precipitated in aqueous slurries, becomes spontaneously to transform into poorly HA [16]. As reported in the literature, the structure of ACP presents the form of either $Ca_9(PO_4)_6 \cdot H_2O$ clusters [17, 18] or $Ca_3(PO_4) \cdot H_2O$, i.e., (TCP)-like [8, 19–21] with bound water.

The TEM micrographs of β-TCP obtained in pure methanol are shown in Fig. 9. It clearly reveals that the dimension of the spherical β-TCP crystal is near 50 nm in diameter (Fig. 9(a)). Furthermore, a high-resolution image of β-TCP oriented along [1 −1 0] zone -axis in Fig. 9(b) clearly displays the regular lattice array. Beside the lattice array region, a thin amorphous region with thickness of about 5–10 nm surrounding the β-TCP crystals was observed. It was believed that the amorphous layer is the PAA, which encapsulates the

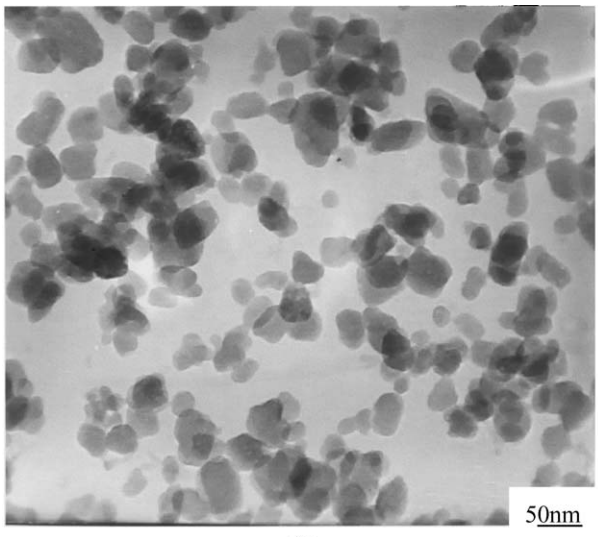

(a)

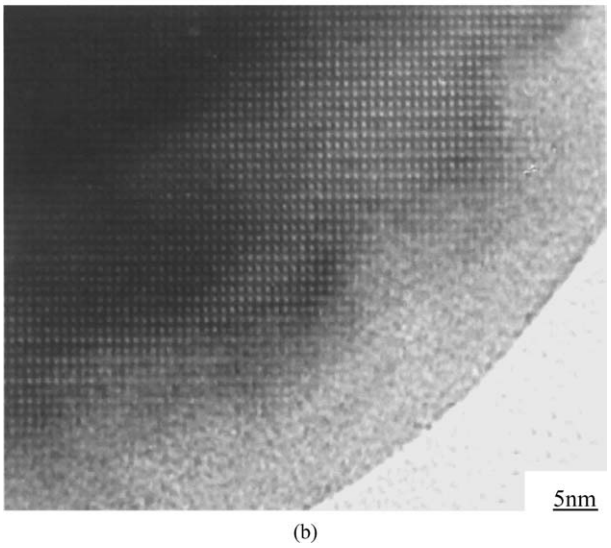

(b)

Figure 9 TEM micrographs of β-TCP: (a) low magnification image and (b) lattice image along [1 −1 0] zone-axis.

nano-crystals by either physical or chemical interaction during synthesis to form a core-shell nanostructured composite.

The amount of water plays an important role on the phase development of calcium phosphate ceramics in the water-methanol mixtures. In other words, as water contained below 10%, ACP easily transforms into β-TCP because of similar crystal structure. On the other hand, above 10% fractional water, both CDHA and ACP phases can be produced as a result of hydrolysis, but the formed phase depends on the fractional methanol and PAA concentrations.

4. Conclusion

In-situ formation of calcium-deficient apatitic (CDHA), amorphous calcium phosphate (ACP) and β-tricalcium phosphate (β-TCP) nanocrystals with a core-shell composite structure were synthesized in the presence of low-molecular-weight poly(acrylic acid) (PAA) and water-methanol (WM) mixtures. The CDHA and β-TCP phases can be well developed in pure water and methanol environment, respectively. However, the crystallinity of both the CDHA and β-TCP decreases with increasing PAA concentrations, indicating the retarding effect of the-PAA molecules on crystal growth. On the other hand, in water-methanol mixtures, low fractional methanol favors the formation of ACP phase at low PAA concentrations, and remains structurally stable with increasing concentration of both methanol and PAA. With more than 50% methanol used, especially between 75 and 90%, the ACP seems hard to develop instead, the CDHA is easily formed particularly with the mixtures of higher fractions of methanol.

Acknowledgement

The authors gratefully acknowledge the National Science Council of the Republic of China for its financial support through Contract No. NSC-91-2216-E-009-025. Thanks also give to ApaMatrix Technologies Inc, Canada, for technical support.

References

1. L. L. HENCH, *J. Amer. Ceram. Soc.* **74** (1991) 1487.
2. D. M. LIU, T. TROCZYNSKI and W. J. TSENG, *Biomaterials* **22** (2001) 1721.
3. K. KATO, Y. EIKA and Y. IKADA, *J. Mater. Sci: Mater. Med.* **32** (1997) 5533.
4. Z. AMJAD, *Phosphorus Res. Bull.* **5** (1995) 1.
5. S. C. LIOU, S. Y. CHEN and D. M. LIU, *Biomaterials* **24** (2003) 3981.
6. C. REICHARDT, "Solvents and Solvent Effects in Organic Chemistry" (VCH, New York, 1988).
7. K. R. HARRIS and P. J. NEWITT, *J. Phys. Chem.* A **103** (1999) 6508.
8. E. LERNER, R. AZOURY and S. SARIG, *J. Cryst. Growth* **97** (1989) 725.
9. S. C. LIOU and S. Y. CHEN, *Biomaterials* **23** (2002) 4541.
10. M. VALLET-REGI, L. M. RODRIGUEZ-LORENZO and A. J. SALINAS, *Solid State Ionic* **101–103** (1997) 1279.
11. J. S. BOW, S. C. LIOU and S. Y. CHEN, *Biomaterials* **25** (2004) 3155.
12. J. CESARMO III and I. A. AKSAY, *J. Amer. Ceram. Soc.* **71**(12) (1998) 1062.
13. V. A. HACKLEY, *ibid.* **80**(9) (1997) 2315.
14. J. L. GREEN, A. R. LACEY and M. G. SCEATS, *Chem. Phys. Lett.* **137**(6) (1987) 537.
15. J. FIDLER and P. M. RODGER, *J. Phys. Chem.* **103** (1999) 7695.
16. F. ABBONA and M. FRANCHINI-ANGELA, *J. Cryst. Growth* **104** (1990) 661.
17. F. BETTS, N. C. BLUMENTHAL and A. S. POSNER, *ibid.* **53** (1981) 63.
18. J. E. HARRIES and D. W. L. HUKINS, *ibid.* **84** (1987) 563.
19. A. NANCOLLAS, in Phosphate Minerals, edited by J. O. Nriagu and P. B. Moore (Berlin/Heidelberg, Springer-Verlag, 1984) p. 137.
20. H. E. LUNDAGER MADSEN, I. LOPEZ-VALERO, V. LOPEZ-ACEVEDO and R. BOISTELLE, *J Cryst. Growth* **75** (1986) 429.
21. S. LAZIC, *ibid.* **147** (1995) 147.

Received 14 November 2003
and accepted 23 June 2004